INSTITUTE OF PHYSICS PUBLISHING JOURNAL OF PHYSICS B: ATOMIC, MOLECULAR AND OPTICAL PHYSICS

J. Phys. B: At. Mol. Opt. Phys. **34** (2001) 4901–4917 PII: S0953-4075(01)27034-5

Study of the transfer ionization process by observing the electron cusp in 100–300 keV He^{2+} + He collisions

L Sarkadi, L Lugosi, K Tőkési, L Gulyás and Á Kövér

Institute of Nuclear Research of the Hungarian Academy of Sciences (ATOMKI), H-4001 Debrecen, PO Box 51, Hungary

Received 17 July 2001, in final form 14 September 2001
Published 26 November 2001
Online at stacks.iop.org/JPhysB/34/4901

Abstract

Cusp-electron emission in He^{2+} on He collisions has been investigated in the energy range 100–300 keV. By detecting the electrons in coincidence with the charge-state-analysed outgoing He^{2+} and He^{+} ions, the processes of electron capture to the continuum (ECC), and ECC accompanied by bound-state capture (transfer ionization, TI) were identified, respectively. The ratios of yields for the TI and ECC cusps are found to increase steeply with decreasing projectile energy. At 100 keV the obtained TI/ECC ratio (1.42 ± 0.14) is almost two times larger than the corresponding ratio measured in a previous experiment for an Ar target at the same impact energy. The measured data are compared with calculations carried out in the independent particle model with use of the classical trajectory Monte Carlo method and the continuum-distorted-wave theory. The disagreement observed between the theory and experiment indicates the presence of electron correlation effects in TI.

1. Introduction

The simultaneous continuum-electron emission and electron transfer is one of the most interesting two-electron (or multiple-electron) processes in the physics of ion–atom collisions. In the last decade this process, called *transfer ionization* (TI), has received a great deal of experimental and theoretical attention. The studies of TI are motivated by the possibility of obtaining information about the role of the electron–electron interaction (correlation) in atomic collisions. As an example, we mention the investigation of the electron correlation in a special type of double-scattering mechanism of charge transfer proposed by Thomas (1927). In this process a target electron is captured by the projectile after successive collisions with the projectile and a second target electron. The second electron recoils with the speed of the projectile ion v_p, resulting in a pronounced peak at about 90° in the angular distribution of the electrons emitted with the matching velocity $v_e = v_p$. The peak, which is an explicit manifestation of a correlated TI process, was observed experimentally in 1 MeV proton on He collisions (Pálinkás *et al* 1989). In a recent experiment (Mergel *et al* 2001) carried out on

the same collision system, further evidence was found for the correlated motion of the emitted and captured electrons in TI; for relatively high collision velocities ($v_p > 2.5$ au) most of the ejected electrons were observed in the backward direction. This surprising finding was interpreted as a result of the strong electron–electron correlation in the initial He ground-state momentum wavefunction.

The subject of this paper is the investigation of TI by observing the so-called cusp electrons. Cusp electrons are emitted in the forward direction and travel with the velocity of the beam of bombarding particles. The velocity (energy) spectrum of these electrons exhibits a cusp-shaped peak centred at $v_e = v_p$ (Crooks and Rudd 1970). The study of TI in this special case of electron emission has the advantage that the enhanced electron yield in the cusp region makes the differential measurement of the process feasible even if the integrated cross section is small.

Since the cusp electrons move very slowly in the projectile-centred reference system, their behaviour is mainly determined by the projectile continuum. Therefore, processes leading to cusp are often called 'electron transfer to the continuum states of the projectile', viewed as a continuation of the bound-state capture into high Rydberg states across the continuum threshold. The cusp-electron emission associated with target ionization is referred to as *electron capture to the continuum* (ECC). In TI the continuum-state capture is accompanied by bound-state capture of an additional electron (or electrons) from the target to the projectile. It is important to note that in this paper we use a restricted meaning of ECC—by definition we mean ECC 'pure' ionization of the target, i.e. cusp-electron emission *without* bound-state capture.

For completeness we should mention that ionization of the projectile (if it is not a fully-stripped ion) may also lead to cusp—in this case the process is called *electron loss to the continuum* (ELC).

This paper is part of a series of systematic investigations dealing with cusp-electron production via TI. The first studies (Závodszky *et al* 1993, Zhu *et al* 1995) were carried out with structured-ion projectiles (He^+, O^{7+}), while later fully-stripped ions (H^+, He^{2+}, O^{8+}) were used (Víkor *et al* 1995, 1997, Plano *et al* 1994, Závodszky *et al* 1995) in order to make the theoretical understanding easier.

The previous experiments carried out in a broad range of collision velocity (from 4.4 keV amu^{-1} to 1.5 MeV amu^{-1}) resulted in a large amount of measuring data. However, until now, a theoretical interpretation of the results has been missing. From the experimental data for TI one can obtain information about the role of the electron–electron interaction only by comparing the measured quantities with theoretical calculations. Unfortunately, the description of the simultaneous capture of two electrons to the bound and continuum states of the projectile is a rather difficult task for the theory, even in the *independent particle model* (IPM). In principle, the IPM cannot be applied to the problem of cusp-electron production via TI without contradiction. The reason is as follows. It is known that the cusp peak is a result of a final-state interaction between the ejected electron and the outgoing projectile (see, for example, Barrachina (1997)), therefore its intensity and shape are determined mainly by the ionic charge of the outgoing projectile. However, in TI the charge state of the projectile changes during the collision due to the bound-state capture, i.e. the incoming charge differs from the outgoing one. The IPM cannot account for this effect, because it treats the ionization and capture as independent processes.

Even if the above problem in connection with the charge state of the outgoing projectile is solved (for example, with the inclusion of the electron–electron interaction), a further difficulty arises for the impact of singly charged ions (e.g. H^+, He^+). In this case the outgoing projectile is a *neutral atom*, and the cusp is formed by a mechanism (Sarkadi *et al* 1989, 1997, Báder

et al 1997) which is completely different from that of cusp production by a charged outgoing projectile. While in the latter case (i.e. for the long-range Coulomb interaction) the cusp formation is well understood theoretically, for the neutral-atom interaction the huge complexity of the problem (Macri and Barrachina 1998, Sarkadi *et al* 2000) prevents a quantitative description.

In most of the previous experiments carried out in our systematic study of TI, an Ar atom was used as the target. From an experimental point of view this choice is justified by the relatively large values of the doubly differential cross section (DDCS) for the electron ejection. On the other hand, Ar is not an ideal atom for theory. The large number of electrons in the outer M shell, as well as the contribution of the inner (K and L) shells to the collision processes make the theoretical treatment difficult. The results of such calculations are rather uncertain because of the applied approximations.

To avoid the above difficulties in the theoretical understanding, we decided to perform an experiment on the simplest collision system for TI. This system is He^{2+} + He. We note that although the collision system H^+ + He is even simpler, in the latter case the outgoing projectile is H^0, i.e. one is faced with the problem of cusp formation by a neutral atom.

For the interpretation of the obtained data we carried out theoretical calculations. The calculations were made in the framework of the IPM by using the classical trajectory Monte Carlo (CTMC) method as well as the continuum-distorted-wave eikonal-initial-state (CDW-EIS) model. To the best knowledge of the authors, the present theoretical work is the first attempt to give a quantitative description of cusp-electron emission by TI.

2. Experimental procedure

The experiment was performed at the 1.5 MV Van de Graaff accelerator of the Institute of Nuclear Research of the Hungarian Academy of Sciences (ATOMKI). The measurement principle is that the cusp-electron production in the different reaction channels is identified by detecting the electrons in coincidence with the outgoing charge-state selected projectiles. For He^{2+} + He collisions the coincidences with the outgoing He^{2+} projectiles identify ECC, i.e. cusp-electron emission without bound-state capture. The coincidences with He^+ identify TI, i.e. cusp-electron emission accompanied by bound-state capture. We note that the ECC channel also contains the (small) contribution of the double ionization of the target.

The experimental set-up was similar to that used in our previous cusp measurements (see, for example, Kövér *et al* (1989), Víkor *et al* (1995)) and will only be briefly described here. The He^{2+} ions, produced by interaction of the He^+ beam of the accelerator with the residual gas of the beam channel, were selected from the original ion beam with a four-stage electrostatic charge-state selector. The energy range of the ions covered a range from 100 to 300 keV. A collimator with a length of 50 cm was used to define the final ion beam of 0.5 mm diameter. To reduce the He^+ contamination of the beam, we mounted an electrostatic beam cleaner (the so-called 'mini cleaner' (Víkor *et al* 1995)) just in front of the gas jet target, following the collimator. The He^+ and He^0 contents of the cleaned He^{2+} beam were less than 0.5 and 0.1%, respectively (without operating the gas target).

The electrons ejected from the target were energy analysed by a double-stage parallel-plate electron spectrometer (Sarkadi *et al* 1998) and counted by a channel electron multiplier (CEM). The spectrometer was characterized by an energy resolution of 6% and an acceptance half-angle of 2°. The outgoing ions were charged-state analysed by means of an electrostatic deflector and detected by a fast particle detector. Standard electronics were used to establish coincidences between the electrons and particles.

We measured the number of coincidence events in the ECC and TI reaction channels and normalized these to the number of the incoming He^{2+} ions and the density of the target atoms. The electron spectra were recorded in the electron velocity range from $0.84v_p$ to $1.16v_p$. The coincidence yield values were corrected for the contribution from the random coincidence events. Furthermore, we checked the contribution due to the fraction of the He^+ ions in the incoming beam for which the final state for ECC is the same as that for TI resulting from He^{2+} impact. In a separate coincidence experiment carried out with a He^+ beam we found the latter contribution negligible.

The measured and corrected electron spectra were divided by the electron energy E to account for the energy dependence of the energy window ΔE of the electron spectrometer. The spectra were also divided by the energy-dependent electron detection efficiency function $\epsilon(E)$. We determined a *relative* $\epsilon(E)$ function in a separate calibration experiment in which we recorded the energy spectrum of electrons (in a range of 0–100 eV) ejected at 0° from collisions of 300 keV protons with He. The obtained data were compared to the tabulated DDCS values of Rudd *et al* (1976). Since the latter data were measured at non-zero emission angles, we had to extrapolate these to 0°. As a check of the extrapolated data, we calculated the corresponding cross sections by using the CDW-EIS theory; good agreement was found. Since the scattering of the theoretical cross sections was much smaller than that of the measured data, finally we used the CDW-EIS results to establish $\epsilon(E)$.

Special care was taken to ensure the single-collision condition. This is a crucial requirement of the TI experiments. If the target is not thin enough, subsequent double (or multiple) collisions may lead to false coincidence yields. For example, let us consider the TI channel in which the electrons are measured in coincidence with the outgoing He^+ ions. The following double collision may contribute to the measured coincidence yield. In the first collision an ECC process takes place, resulting in the cusp electron. Then the outgoing He^{2+} ion captures an electron in the second collision with *another* target atom, resulting in the outgoing He^+ ion.

The probability of the double (multiple) scattering increases with the target pressure, therefore one can check the single-collision condition repeating the measurement at different values of the target pressure. Figure 1 shows the result of such an experiment carried out at 200 keV impact energy. In the figure are plotted the ratios of the number of coincidences to that of the 'singles' events as a function of the target pressure (more precisely, the difference $p - p_0$, where p and p_0 are pressures with and without the target gas, respectively). In this test experiment, the voltage of the electron spectrometer was tuned to the cusp maximum. As is seen from figures 1(*a*) and (*b*), the ECC and TI yields (coincidences with He^{2+} and He^+, respectively) are not affected by double collisions. At the same time, a strong pressure dependence was found for the yield of coincidences with He^0 (figure 1(*c*)). This latter finding is understandable, because the capture of two electrons with simultaneous electron ejection would be a three-electron process that cannot happen for a He target. Consequently, the observed coincidences with He^0 originated from double collisions.

3. Results and discussion

3.1. Experimental data

Figure 2 shows typical electron spectra obtained at 130 keV impact energy. A striking feature of the figure is the surprisingly large contribution of TI to the total cusp; the amplitude of the TI cusp roughly agrees with that of the ECC cusp. The TI cusp is almost symmetric whereas, in contrast, the ECC cusp is strongly asymmetric. The latter peak is shifted by about 1 eV

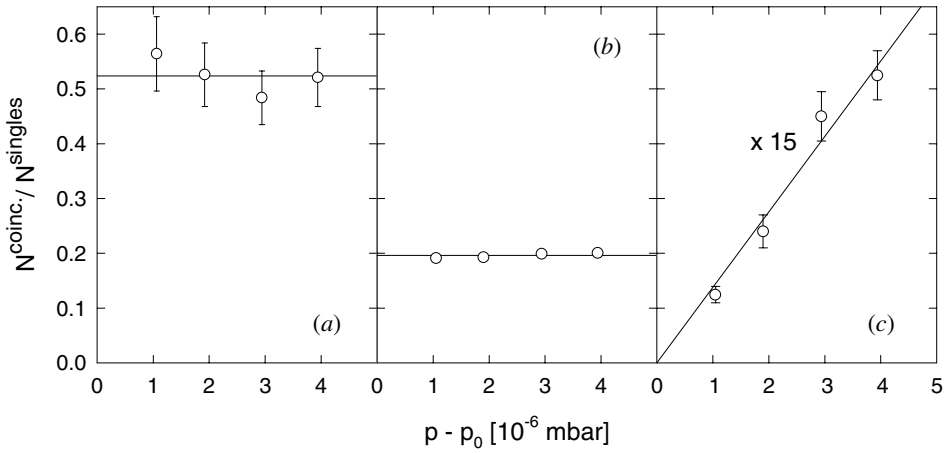

Figure 1. Coincidence to single yield ratio of the cusp electrons as a function of the pressure of the target gas. The measurements were made at 200 keV impact energy. The electron spectrometer was tuned to the cusp maximum. (*a*)–(*c*) correspond to coincidence detection of the electrons with the outgoing He^{2+} (ECC), He^{+} (TI) and He^{0} particles, respectively.

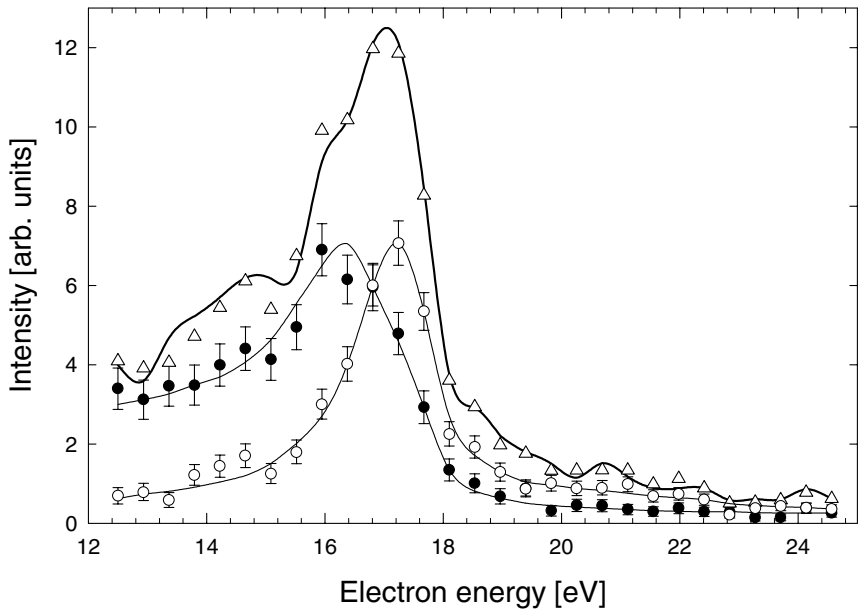

Figure 2. Cusp-electron energy spectra measured in 130 keV He^{2+} + He collisions: full circles, coincidences with He^{2+} (ECC); open circles, coincidences with He^{+} (TI); triangles, sum of the coincidence spectra; thick curve, 'singles' electron spectrum. The thin curves through the coincidence data are drawn only to guide the eye.

to lower energy. We note that the shift can probably be explained (Tőkési *et al* 1997) by the asymmetry of the peak taking into account the finite energy and angular resolution of the measurement. Due to the different shapes of the ECC and TI cusps, the 'singles' electron spectrum is structured. One can clearly see that it is composed of two peaks: a narrow peak is superimposed on a broader peak. The bump seen at the low-energy side of the narrow peak at about 16 eV is due to the shifted maximum of the ECC cusp.

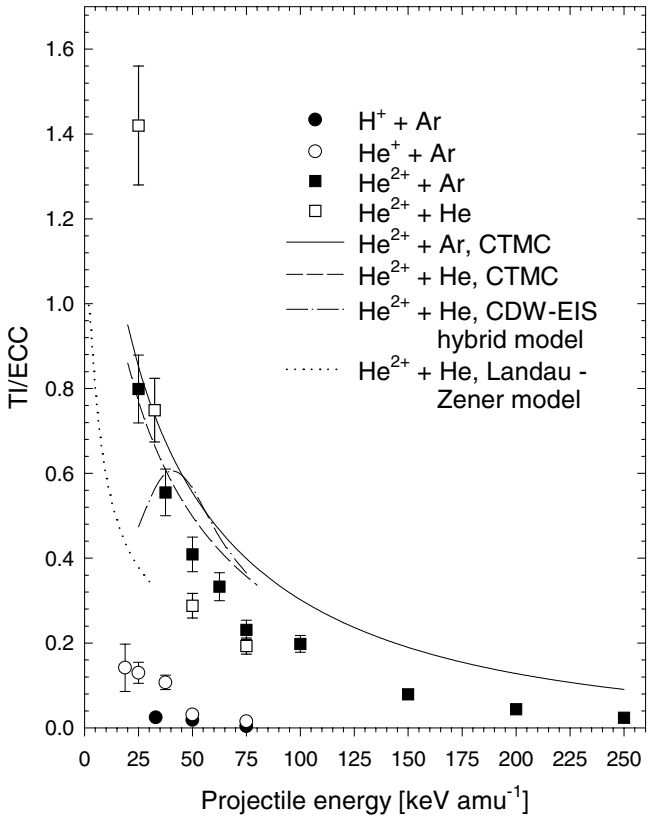

Figure 3. Cusp-electron production by TI relative to ECC as a function of the impact energy. The notations of the experimental data are as follows: full circles, proton on Ar (Víkor *et al* 1995); open circles, He^+ on Ar (Závodszky *et al* 1993); full squares, He^{2+} on Ar (Víkor *et al* 1997); open squares, He^{2+} on He (present work). The notations of the theoretical curves are as follows. The solid curve represents the CTMC model for He^{2+} on Ar collisions. He^{2+} on He collisions: dashed curve, CTMC; dashed-dotted curve, CDW-EIS hybrid model; dotted curve, Landau–Zener model.

As in our previous TI studies, our primary aim was to determine the *ratios* of the cusp-electron production cross sections for the TI and ECC channels. The TI/ECC ratio is an interesting quantity, because it is a measure of the strength of the two-electron over the single-electron process. One may assume that this ratio is sensitive to electron correlation effects.

To establish the TI/ECC ratios from the measured data, we determined relative *singly* differential cross sections (SDCS) integrating the coincidence spectra over the electron energy range. The obtained ratios are plotted in figure 3 as a function of the impact energy. The error of the data was estimated from the results of repeated measurements that reproduced the TI/ECC ratios within 10%. The main source of this error was the uncertainty of the particle detection efficiency.

The new He^{2+}+He data are presented along with the results obtained in previous works for an Ar target with H^+ (Víkor *et al* 1995), He^+ (Závodszky *et al* 1993) and He^{2+} (Víkor *et al* 1997) projectiles. Interestingly, the TI/ECC ratios for He^{2+} impact show only a small dependence on the target, except for the data at the lowest energy, 25 keV amu^{-1}. This is surprising, because one would expect that the probability of the two-electron TI process (compared to the single-electron ECC) would be considerably larger for the many-electron Ar than for He.

It is even more surprising that at 25 keV amu^{-1} (100 keV total energy) a very large value, 1.42 ± 0.14, was obtained for the TI/ECC ratio in the present experiment. This value is larger by almost a factor of two than that measured for the Ar target at the same impact energy. The fact that, in 100 keV He^{2+} + He collisions, TI considerably exceeds ECC means that in the majority of cusp-electron emissions the process is accompanied by a bound-state capture. This is in contradiction with the general view that the one-electron process should be much stronger than the two-electron process.

To confirm the above unexpected result, we checked our experimental procedure repeating the old measurement on an Ar target at 100 keV. The re-measured value of the TI/ECC ratio, 0.712 ± 0.070, is slightly smaller than the old value, 0.799 ± 0.080, but the deviation is within the errors. This check was important, because the experimental set-up was not completely identical in the two measurements. In the old measurement a high-resolution double-stage cylindrical mirror electron spectrometer was used, and the electrons were accelerated by an electrostatic lens before analysis (Víkor *et al* 1996).

3.2. Theory

As was mentioned in the introduction, we used the IPM for the interpretation of the obtained experimental data. The IPM reduces the description of the many-electron collision system to that of a three-body system consisting of the projectile, an active electron and the target atom. The role of the passive electrons of the target and/or projectile ion is taken into account by an effective potential.

For the calculation of the cross section of a multi-electron process (such as TI) the most straightforward approach is the impact-parameter formulation of the scattering problem. In this method one determines impact-parameter-dependent one-electron probabilities, and the products of these quantities are used to express the probabilities of the many-electron processes. For a three-body collision system, the basic one-electron probabilities are those for capture, ionization and excitation, denoted by p_c, p_i and p_e, respectively. If by definition p_c is the sum of the capture probabilities to all bound states of the projectile, p_i is an integrated ionization probability over the energy and emission angle of the ejected electron, and p_e is the excitation probability to all bound states of the target (including the initial ground state), then the relation $p_c + p_i + p_e = 1$ holds. For the characterization of the continuum-electron emission we introduce the doubly differential one-electron ionization probability $d^2 p_i/dE\, d\Omega$ which is related to p_i at a fixed value of the impact parameter b by

$$\int_E \int_\Omega \frac{d^2 p_i}{dE\, d\Omega}\, dE\, d\Omega = p_i(b). \tag{1}$$

By using the quantities defined above, one can derive expressions for the doubly differential ionization probabilities (and cross sections) of the simultaneous ionization and capture of electrons from a *many-electron* atom. The general expressions and results for the special cases of ECC and TI are given in the appendix.

For the calculation of the one-electron ionization and capture probabilities, we used the CTMC method (Abrines and Percival 1966, Olson and Salop 1977). The method is based on the numerical solution of Newton's classical equations of motion for a large number of trajectories under randomly chosen initial conditions. The CTMC method has the advantage that it treats the three-body (many-body) dynamics exactly. This is particularly important for the description of the cusp-electron production where one has to take into account the long-range Coulomb interaction in the final state between the scattered ion, the emitted electron and the recoil ion on equal footing (see, for example, Garibotti and Miraglia (1980)).

The calculations were made for a He^{2+} projectile and for both He and Ar targets. The many-electron target atom was replaced by a one-electron atom, representing the ion core by a model potential developed by Green *et al* (1969) based on Hartree–Fock calculations. The potential has the following form for a neutral atom (in atomic units)

$$V(r) = -[(Z-1)\Omega(r)+1]/r \tag{2}$$

where Z is the nuclear charge and

$$\Omega(r) = \{(\eta/\xi)[\exp(\xi r)-1]+1\}^{-1}. \tag{3}$$

The values of η and ξ were taken from Garvey *et al* (1975). For He $\eta = 1.77$ and $\xi = 2.625$; for Ar $\eta = 3.50$ and $\xi = 0.957$.

Concerning the choice of the random initial parameters, we followed the procedure proposed by Reinhold and Falcón (1986) for non-Coulombic interaction. These authors applied a three-body CTMC model to describe the H^+ + He collision. In one of the versions of their model they represented the He^+ core by the following model potential

$$V_{\rm mod}(r) = -[Z-1+(1+Z_{\rm eff}r)\exp(-2Z_{\rm eff}r)]/r \tag{4}$$

where $Z_{\rm eff} = Z - \frac{5}{16}$. We compared this potential with that given by equations (2) and (3) for He. An excellent agreement was found. This means that our CTMC method is equivalent to that of Reinhold and Falcón (1986). As a check of our CTMC computer code we repeated the total cross-section calculations of these authors for the single ionization, free-electron production, single capture and double ionization in collisions of protons with He atoms. The test was made at 100 keV impact energy. Our results agreed well with those of Reinhold and Falcón.

For the collision systems He^{2+} + He, He^{2+} + Ar we made the calculations in two steps. In the first step, the equations of motion were integrated until the main reaction channels (excitation, ionization, electron capture to bound states of the projectile) were well separated. This condition was fulfilled at an internuclear distance of 25 au. In the second step, only collision events leading to ionization were regarded. Since the cusp is a result of final-state interaction between the ionized electron and the outgoing projectile, to achieve convergence the equations of motion in the final ionization channel had to be integrated over a large internuclear separation. In the present work the integration was stopped at 10^5 au. Details of the treatment of the electron cusp by means of the CTMC method can be found in previous works (Tőkési and Mukoyama 1994, Tőkési *et al* 1997, Sarkadi *et al* 2000).

From the trajectory calculations we obtained DDCSs for the ECC and TI cusps in the following way. First let us consider the *one-electron* DDCS for ionization (i.e. DDCS for electron ejection in the three-body collision system)

$$\frac{{\rm d}^2\sigma_i}{{\rm d}E\,{\rm d}\Omega} = 2\pi\int_0^\infty b\frac{{\rm d}^2p_{\rm i}(b)}{{\rm d}E\,{\rm d}\Omega}\,{\rm d}b. \tag{5}$$

This expression in CTMC is approximated by

$$2\pi\int_0^\infty b\frac{{\rm d}^2p_{\rm i}(b)}{{\rm d}E\,{\rm d}\Omega}\,{\rm d}b \approx \frac{b_{\rm max}\sum_j b_j^{(i)}}{N(\cos\vartheta_{\rm min}-\cos\vartheta_{\rm max})\Delta E} \tag{6}$$

where N is the total number of trajectories calculated in the impact parameter range $(0, b_{\rm max})$, $b_j^{(i)}$ is the actual impact parameter when the criterion for ionization is fulfilled, ΔE is the energy window, and $2\pi(\cos\vartheta_{\rm min}-\cos\vartheta_{\rm max})$ is the solid angle window for the ejected electron.

For a many-electron target atom, the expression of DDCS for ECC and TI (denoted by ${\rm d}^2\sigma_{c^0}/{\rm d}E\,{\rm d}\Omega$ and ${\rm d}^2\sigma_{c^1}/{\rm d}E\,{\rm d}\Omega$, respectively) is given by equation (A.9). Using equations (A.3) and (A.5) we can write equation (A.9) as follows

$$\frac{{\rm d}^2\sigma_{c^{0,1}}}{{\rm d}E\,{\rm d}\Omega} = 2\pi\int_0^\infty b\frac{{\rm d}^2p_{\rm i}(b)}{{\rm d}E\,{\rm d}\Omega}f_{c^{0,1}}(b)\,{\rm d}b \tag{7}$$

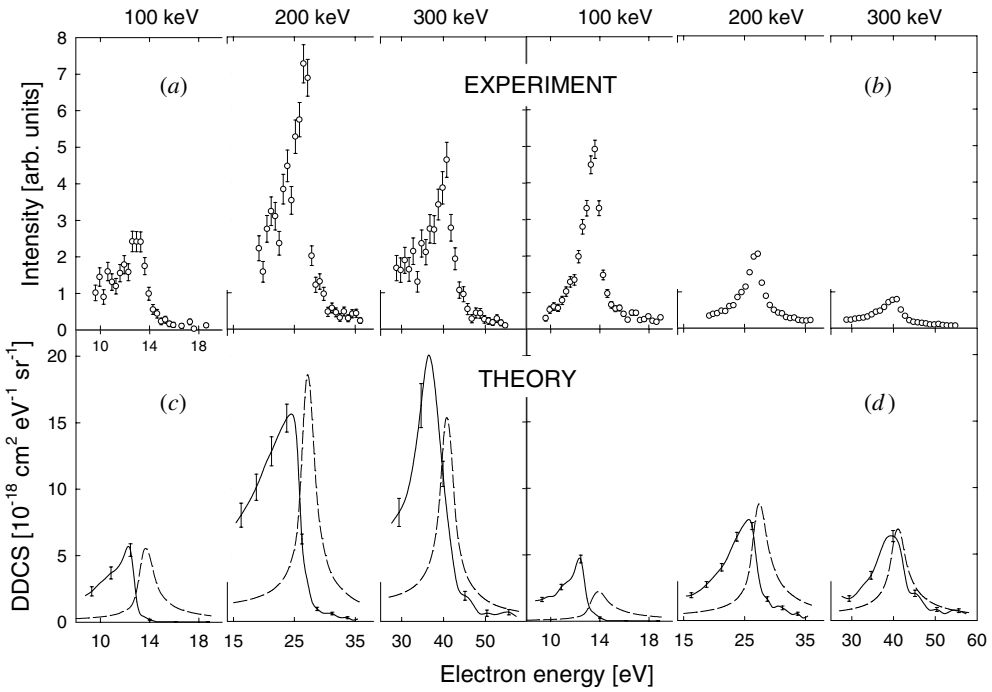

Figure 4. Measured and calculated cusp-electron spectra for He^{2+} + He collisions at 100, 200 and 300 keV impact energies: (*a*) and (*c*) ECC spectra; (*b*) and (*d*) TI spectra. Notations of the theories: solid line, CTMC; dashed line, CDW-EIS hybrid model.

where

$$f_{c^0} = \frac{1}{p_i}\left[(p_i + p_e)^N - p_e^N\right] \tag{8a}$$

$$f_{c^1} = \frac{1}{p_i} N p_c \left[(p_i + p_e)^{N-1} - p_e^{N-1}\right]. \tag{8b}$$

Comparing equation (7) with equations (5) and (6), we may write the following modified CTMC cross-section formula for ECC and TI

$$\frac{d^2\sigma_{c^{0,1}}}{dE\, d\Omega} \approx \frac{b_{max} \sum_j b_j^{(i)} f_{c^{0,1}}(b_j^{(i)})}{N(\cos\vartheta_{min} - \cos\vartheta_{max})\Delta E}. \tag{9}$$

To achieve a satisfactory statistical accuracy of DDCSs in the cusp region, the integration of $(2-15)\times 10^6$ trajectories was required, depending on the collision velocity and target atom. The calculated electron spectra for the TI and ECC cusps are compared with the experimental spectra in figure 4. The target is He. The presented spectra belong to 100, 200 and 300 keV impact energies. We note that, although we did not determine absolute cross sections in the experiment, the measured data in the figure show a correct *relative* energy dependence of the cusp intensity as a function of the impact energy. The experimental energy dependence is not reproduced by the CTMC theory. For ECC a maximum of the cusp intensity was found in the experiment at about 200 keV. At the same time, CTMC predicts that the intensity of the ECC cusp increases with the impact energy in the regarded region. Concerning the TI cusp, the experimental data show a monotonic decrease of the peak with increasing energy, while the CTMC results indicate a broad maximum around 200 keV. The observed cusp shapes are more

or less reproduced by the theory, although the TI cusp obtained from the CTMC simulation is not as sharp and symmetric as the measured one, particularly at low impact energy.

CTMC is a classical description, and the question of neglecting possible quantum effects arises. This motivated us to also perform quantum mechanical calculations. For this purpose we used the CDW-EIS model (Crothers and McCann 1983) which is known to be a very efficient theory for the description of the continuous electron ejection in ion–atom collisions (see, for example, Fainstein *et al* (1991)). The ejected electron is described by a two-centre wavefunction, therefore the model gives an account of the cusp-electron emission. We made the calculations again in the IPM. The applied CDW-EIS model (Fainstein *et al* 1996) assumes a straight-line trajectory for the projectile path and uses Hartree–Fock wavefunctions for the initial and final electronic states. Since CDW-EIS is a perturbation theory, it works only when the probability of the regarded process is small. This holds for ionization. In contrast to this, in low-energy He^{2+} + He collisions the probability of the electron capture may take values close to 1 (see later), and CDW-EIS is unreliable. To avoid this problem, we combined CDW-EIS with CTMC: the one-electron doubly differential ionization probabilities were obtained by the CDW-EIS model, and CTMC was used to calculate the electron capture probabilities. In the following, the combined theory will be referred to as the 'CDW-EIS hybrid model'.

The electron spectra predicted by the hybrid model are plotted in figure 4. On average, the intensities of the cusp peaks obtained by the classical simulation and the combined quantum–classical mechanical description agree surprisingly well. Unlike CTMC, the hybrid model predicts a maximum of the ECC cusp around 200 keV, in qualitative agreement with the experiment. For the TI cusp, the hybrid model provides an even worse description than CTMC, largely underestimating the intensity of the cusp at 100 keV impact energy.

The hybrid model predicts practically symmetric cusp shapes for both ECC and TI, in contradiction with the experiment and CTMC. However, CTMC seems to predict too large an asymmetry for the ECC cusp—this causes a larger energy shift of the peak than that observed experimentally.

The reason for the asymmetry of the ECC cusp is well known. It can be explained by a two-centre effect: the electron focused in the forward direction by the outgoing projectile is slightly decelerated as a result of interaction also with the ionized target. By using CTMC, we have tried to understand why the TI cusp is symmetric. In this analysis we started out from the integral occurring in the expression (A.9) of DDCS. For a He target atom, the form of the integral is as follows (apart from constant factors)

$$\int_0^\infty b\frac{\mathrm{d}^2 p_\mathrm{i}(b)}{\mathrm{d}E\,\mathrm{d}\Omega}p_\mathrm{c}(b)\,\mathrm{d}b. \tag{10}$$

To simplify the analysis, instead of DDCS we regarded the integrated cross section for the TI cusp, i.e. we analysed the integral $\int_0^\infty bp_\mathrm{i}^\mathrm{cusp}(b)p_\mathrm{c}(b)\,\mathrm{d}b$ where $p_\mathrm{i}^\mathrm{cusp}(b)$ is the one-electron cusp-production probability

$$p_\mathrm{i}^\mathrm{cusp}(b) = \int_{E_1}^{E_2}\int_{\Delta\Omega}\frac{\mathrm{d}^2 p_\mathrm{i}(b)}{\mathrm{d}E\,\mathrm{d}\Omega}\mathrm{d}E\,\mathrm{d}\Omega. \tag{11}$$

Here $\Delta\Omega$ is the solid angle in which the electrons are detected. E_1 and E_2 define the range of the electron energy where the cusp peak is measured (see section 2). In figure 5 we plotted the functions $bp_\mathrm{i}^\mathrm{cusp}(b)$ and $p_\mathrm{c}(b)$ for 100 and 300 keV impact energies. As a comparison we also plotted $bp_\mathrm{i}(b)$, where $p_\mathrm{i}(b)$ is the total ionization probability. A striking feature of the figure is that the impact-parameter dependence of the cusp-production probability strongly differs from that of the the total ionization probability. Besides the maximum seen for both $bp_\mathrm{i}(b)$ and $bp_\mathrm{i}^\mathrm{cusp}(b)$ at small impact parameters ($\leqslant$1 au), for the function

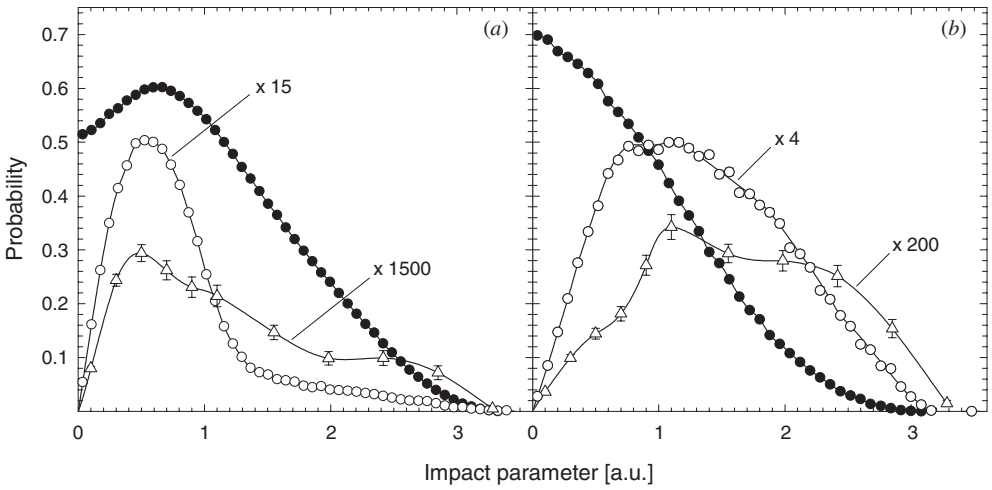

Figure 5. The functions entering in the integral expression of the cross section for the cusp production by TI at (*a*) 100 keV and (*b*) 300 keV impact energies. The displayed data are the results of CTMC calculations: full circles, $p_c(b)$; open triangles, $bp_i^{cusp}(b)$. As a comparison the function $bp_i(b)$ is also plotted (open circles). $p_c(b)$, $p_i^{cusp}(b)$ and $p_i(b)$ are the probabilities of electron capture, cusp production and total ionization, respectively. The curves through the data are drawn only to guide the eye.

$bp_i^{cusp}(b)$ one can observe an enhancement also at large impact parameters. The maximum located at small impact parameters (which can be understood in terms of the so-called *Massey criterion*) and the bump occurring at about 2.5 au indicate two different mechanisms of cusp formation.

In figure 6 the cusp-electron spectra belonging to the two impact-parameter regions discussed above are seen for a 300 keV impact energy. The two spectra were obtained evaluating the one-electron DDCSs with the use of expression (6) separately for impact parameters $b_j^{(i)} < 1.5$ au and $b_j^{(i)} > 1.5$ au. The cusp belonging to small impact parameters is narrow and symmetric. For large impact parameters we obtained a peak which is strongly asymmetric and shifted towards low energies. We call attention to the great similarity between the shapes of these spectra and those of the experimental energy distributions seen in figure 2.

The dependence of the cusp shape on the impact parameter found in the CTMC simulation explains why the observed TI cusp is narrow and symmetric. In the integral given by equation (10) $b\,\mathrm{d}^2p_i(b)/\mathrm{d}E\,\mathrm{d}\Omega$ is weighted by the capture probability $p_c(b)$. The latter function is strongly peaked at small impact parameters. This means that in the integral the contribution of the narrow and symmetric peak is enhanced.

Now the question remains: what is the physics of cusp production leading to different peak shapes at small and large impact parameters? To answer this question one has to analyse the individual electron trajectories for collision events contributing to the cusp in the different regions of the impact parameter. Such an investigation is beyond the scope of this paper.

Concerning the TI/ECC cusp intensity ratios, the predictions of the CTMC model are compared with the experimental data for both He and Ar targets in figure 3. The agreement is only qualitative. CTMC cannot reproduce the steep increase of the experimental TI/ECC ratio data for a He target with decreasing projectile energy. In the figure we have also plotted the results obtained by the CDW-EIS hybrid model for a He target. This model predicts a decline of the TI/ECC ratio at small impact energies, in complete disagreement with both the

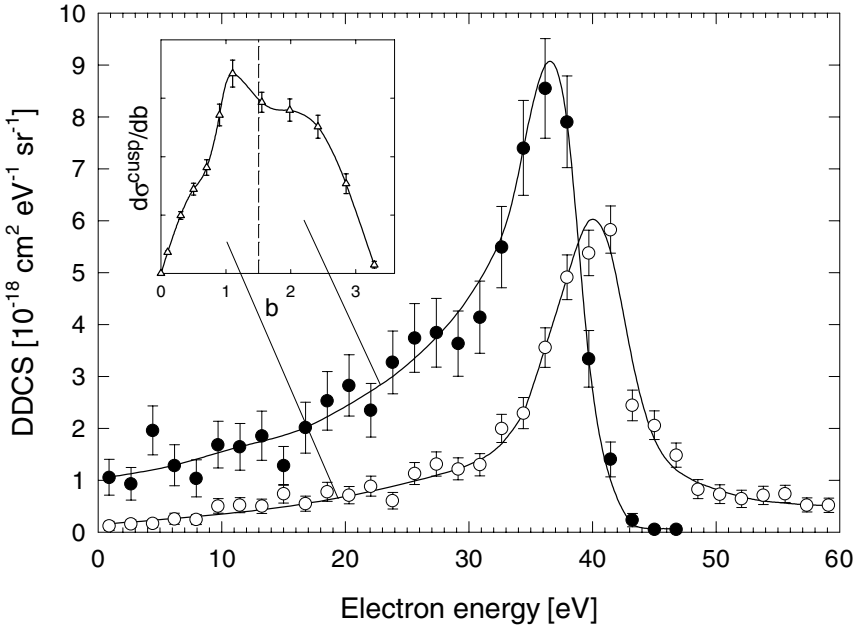

Figure 6. Cusp-electron spectra belonging to two different impact-parameter regions (open circles, $b_j^{(i)} < 1.5$ au; full circles, $b_j^{(i)} > 1.5$ au). The data are one-electron DDCSs obtained from CTMC calculations. The impact energy is 300 keV. The inset shows the selected regions of the impact parameter repeating the curve $bp_{\rm i}^{\rm cusp}(b)$ of figure 5 for cusp production.

experiment and the CTMC simulation.

The poor performance of both the CTMC simulation and the CDW-EIS hybrid model indicates the failure of the IPM in describing the cusp-electron production by TI. However, the limited validity of these theories due to the applied approximations does not allow us to conclude that electron correlation may be a reason for the disagreement. Therefore, we carried out a further theoretical analysis. The large value of the TI/ECC ratio obtained in our experiment for 100 keV He^{2+} + He collisions has motivated us to investigate the question: what is the maximum value of the TI/ECC ratio that can be obtained in the IPM in the region of small impact energies? For low-energy collisions $p_{\rm i} \ll p_{\rm e}$ holds, therefore we can apply the approximate doubly differential probabilities given by equations (A.6*a*) and (A.6*b*) to determine the cusp-production cross sections for ECC and TI. Also using equations (A.9) and (11) we obtain

$$\sigma_{\rm ECC} = \int_{E_1}^{E_2} \int_{\Delta\Omega} \frac{{\rm d}^2\sigma_{c^0}}{{\rm d}E\,{\rm d}\Omega}\,{\rm d}E\,{\rm d}\Omega \approx 2\pi \int_0^\infty bNp_{\rm i}^{\rm cusp}(b)\,[1-p_{\rm c}(b)]^{N-1}\,{\rm d}b \tag{12a}$$

$$\sigma_{\rm TI} = \int_{E_1}^{E_2} \int_{\Delta\Omega} \frac{{\rm d}^2\sigma_{c^1}}{{\rm d}E\,{\rm d}\Omega}\,{\rm d}E\,{\rm d}\Omega \approx 2\pi \int_0^\infty bN(N-1)p_{\rm i}^{\rm cusp}(b)p_{\rm c}(b)\,[1-p_{\rm c}(b)]^{N-2}\,{\rm d}b. \tag{12b}$$

The ratio of the cross sections

$$\frac{\sigma_{\rm TI}}{\sigma_{\rm ECC}} \approx (N-1)\frac{\int_0^\infty bp_{\rm i}^{\rm cusp}(b)p_{\rm c}(b)\,{\rm d}b}{\int_0^\infty bp_{\rm i}^{\rm cusp}(b)[1-p_{\rm c}(b)]\,{\rm d}b}. \tag{13}$$

Let us assume that $p_{\rm c}(b)$ varies slowly in that region of the impact parameters where the product $bp_{\rm i}^{\rm cusp}(b)$ takes appreciable values. From figure 5 one can see that this assumption

is valid at low impact energies. This means that $p_c(b)$ in equation (13) can be replaced by a constant. We can obtain an upper limit for the TI/ECC ratio, if we choose the constant as the maximum of the $p_c(b)$ function, p_c^{max}

$$\left(\frac{\sigma_{TI}}{\sigma_{ECC}}\right)^{\text{upper limit}} = (N-1)\frac{p_c^{max}}{1-p_c^{max}}. \tag{14}$$

For low-energy He^{2+}+ He collisions the value of p_c^{max} can be estimated qualitatively. According to the *classical potential barrier model* (for a review see, for exmaple, Cocke (1993)), the target electron may freely transfer to the projectile at such a sufficiently small internuclear distance where the potential barrier formed by the superposition of the Coulomb fields of the projectile ion and the target core is less than the Stark-shifted ionization potential of the target. Due to the symmetry of the He^{2+} + He collision, in the final state the electron will be found with equal probability on either the projectile or the target, i.e. $p_c^{max} = 0.5$. (For a more accurate estimation of p_c^{max} one has to take into account that the He^{2+}+He system is slightly asymmetric because of the partially screened Coulomb potential of the He^+ core.)

With $p_c^{max} = 0.5$ equation (14) for a He target ($N = 2$) yields a value of 1 for the upper limit of the TI/ECC ratio in the IPM. Since the measured value 1.42 ± 0.14 at 100 keV is considerably larger than 1, we may conclude that the cusp production via TI in the low-energy He^{2+} + He collisions is probably influenced by electron correlation effects.

As an attempt at a quantitative determination of p_c^{max} for the He^{2+} +He system we used the Landau–Zener model in the framework of the molecular-orbital (MO) description of atomic collisions. Details of these calculations will be published elsewhere; here we summarize only the main points of the applied procedure. The H_{12} off-diagonal matrix element of the potential coupling at the crossing point of the MO states was calculated by using the universal formula given by Olson and Salop (1976). The crossing distance R_c was determined by using MO energy terms that were derived applying second-order perturbation theory (Landau and Lifshitz 1975). The trajectory of the projectile was approximated by a straight line.

At small collision velocities the Landau–Zener model resulted in $p_c^{max} \approx 0.5$, in accordance with the value obtained from our qualitative estimation. Replacing the calculated p_c^{max} values in equation (14) we determined an upper limit of the TI/ECC ratio as a function of the impact energy. The result of the Landau–Zener calculations is seen in figure 3. At very low impact energy the curve reaches a maximum with $\sigma_{TI}/\sigma_{ECC} \approx 1$, i.e. we may conclude again that in the IPM the TI/ECC ratio for He^{2+} +He collisions cannot take values significantly larger than 1.

We note that, according to equation (14), the TI/ECC ratio becomes infinite when p_c^{max} approaches 1. It is well known that in slow collisions of highly charged heavy ions with neutral atoms the probability of charge transfer is close to 1. Consequently, in such collisions the TI/ECC ratio can take very large values, even in the IPM. This is in accordance with the results of previous experiments (Tanis *et al* 1990, Plano *et al* 1994) carried out with very low-energy highly charged heavy ions (3.8 keV amu^{-1} O^{6+}, 4.4 keV amu^{-1} O^{8+}). The main conclusion of these works was that low-energy continuum-electron emission at 0° is nearly *always* accompanied with bound-state capture of one or more electrons.

4. Conclusions and outlook

We investigated the TI process by observing the cusp electrons in He^{2+}+He collisions at small impact energies. We compared the two-electron TI with the single-electron ECC. We found that the TI/ECC ratio steeply increases with decreasing collision energy, and at the lowest energy point of the measurement it significantly exceeds 1. CTMC and CDW calculations

carried out in the IPM failed to explain the large probability of TI. In an analysis within the classical potential barrier model and the Landau–Zener theory we established an upper limit for the TI/ECC ratio in the IPM at small impact energies. The conclusion of this analysis was that TI in the low-energy $He^{2+}+He$ collisions is probably influenced by electron correlation effects.

For a better understanding of the process, the inclusion of the electron–electron interaction in the theoretical descriptions is required. Keeping in mind that the treatment of the electron cusp even in the IPM is rather difficult due to the three-body character of this special kind of electron emission (see, for example, Fiol *et al* (2001)), the exact solution of the four-body quantum mechanical problem of TI cannot be expected in the near future. At present, four-body CTMC calculations seem to be feasible. However, a serious difficulty arises in CTMC when the electron–electron interaction is included. It is well known that the classical two-electron (many-electron) system (e.g. the He atom) is unstable because, due to the energy exchange between the electrons, it shortly 'decays' by an autoionization-like process. The autoionization can be prevented by an appropriate simulation of the repulsing Heisenberg core that ensures the stability of the quantum mechanical two-electron (many-electron) system. Although in such an approach the question of neglecting possible quantum effects would still remain, by inclusion of the electron–electron interaction one could take into account the change of the projectile charge during the collision, as well as the difference between the ionization potentials for the removal of one and two electrons from the He atoms. These two effects probably have a deciding role in the cusp-electron production via TI.

To explore the cusp formation further, a possible step would be the experimental verification of the structure found in our CTMC calculations for the impact-parameter dependence of the cusp-production probability. Such measurements for the cusp have already been made by using light- and heavy-ion projectiles (Jagutzki *et al* 1991, Skutlartz *et al* 1988), but at higher impact energies ($\approx$0.5 MeV amu^{-1}) and in the range of smaller impact parameters ($b < 0.5$ au). An experimental investigation of the impact-parameter dependence would help to understand the difference between the shapes of the ECC and TI cusps observed in the present work.

Acknowledgments

This work was supported by the Hungarian Scientific Research Foundation (OTKA, grant nos T 031833 and T 032306). One of the authors (KT) was also supported by the Hungarian Ministry of Culture and Education (grant 'Magyary'). LG gratefully acknowledges the grant from the J Bolyai Research Scholarship.

Appendix. IPM expressions for the simultaneous ionization and electron capture

Let us consider the simultaneous ionization and capture of electrons from a many-electron atom. For the sake of simplicity we assume that the process takes place from *one* atomic shell (for example, the outer shell) having N identical electrons. Denoting the configuration of the ionization of n electrons and capture of m electrons by $i^n c^m$, we can express the differential ionization probability of the electron emission as follows

$$\frac{\mathrm{d}^{2n}P_{i^n c^m}}{\mathrm{d}E_1\,\mathrm{d}\Omega_1\,\mathrm{d}E_2\,\mathrm{d}\Omega_2\ldots\mathrm{d}E_n\,\mathrm{d}\Omega_n} = \binom{N}{n}\binom{N-n}{m}\frac{\mathrm{d}^2p_\mathrm{i}}{\mathrm{d}E\,\mathrm{d}\Omega}\Big|_{E_1\Omega_1}\times\frac{\mathrm{d}^2p_\mathrm{i}}{\mathrm{d}E\,\mathrm{d}\Omega}\Big|_{E_2\Omega_2} \times\cdots\times\frac{\mathrm{d}^2p_\mathrm{i}}{\mathrm{d}E\,\mathrm{d}\Omega}\Big|_{E_n\Omega_n}\times p_\mathrm{c}^m\,p_\mathrm{e}^{N-(n+m)}. \tag{A.1}$$

This is a $2n$ times differential probability that can be used for a process where the energy and emission angle of each ejected electron are measured. If only one of the ionized electrons is detected (as in the present experiment), the doubly differential ionization probability is given by

$$\frac{\mathrm{d}^2 P_{i^n c^m}}{\mathrm{d}E\,\mathrm{d}\Omega} = \binom{N}{n}\binom{N-n}{m}\frac{\mathrm{d}^2 p_\mathrm{i}}{\mathrm{d}E\,\mathrm{d}\Omega} p_\mathrm{i}^{n-1} p_\mathrm{c}^m p_\mathrm{e}^{N-(n+m)}. \tag{A.2}$$

We call attention to the fact that we use small 'p' and capital 'P' to distinguish between the one-electron probabilities obtained directly from the solution of the three-body scattering problem and the probabilities characterizing the collision processes in the many-electron system, respectively.

Now we derive expressions for ECC and TI. We introduce the notation $\mathcal{P}_{c^m}$ for the *inclusive* probability of ionization of any number of electrons together with the simultaneous capture of m electrons. For ECC $m = 0$, therefore using equation (A.2) we can write

$$\begin{aligned}\frac{\mathrm{d}^2\mathcal{P}_{c^0}}{\mathrm{d}E\,\mathrm{d}\Omega} &= \sum_{n=1}^{N}\frac{\mathrm{d}^2 P_{i^n c^0}}{\mathrm{d}E\,\mathrm{d}\Omega} = \frac{\mathrm{d}^2 p_\mathrm{i}}{\mathrm{d}E\,\mathrm{d}\Omega}\sum_{n=1}^{N}\binom{N}{n}\binom{N-n}{0} p_\mathrm{i}^{n-1} p_\mathrm{e}^{N-n} \\ &= \frac{\mathrm{d}^2 p_\mathrm{i}}{\mathrm{d}E\,\mathrm{d}\Omega}\frac{1}{p_\mathrm{i}}\left[(p_\mathrm{i}+p_\mathrm{e})^N - p_\mathrm{e}^N\right].\end{aligned} \tag{A.3}$$

Here we have used the binomial relationship

$$(a+b)^n = \sum_{k=0}^{n}\binom{n}{k} a^k b^{n-k}.$$

In the TI process studied in this paper, the ionization is accompanied by the capture of one target electron, i.e. $m = 1$. The maximum number of ionized electrons is $N-1$, therefore we can write

$$\frac{\mathrm{d}^2\mathcal{P}_{c^1}}{\mathrm{d}E\,\mathrm{d}\Omega} = \sum_{n=1}^{N-1}\frac{\mathrm{d}^2 P_{i^n c^1}}{\mathrm{d}E\,\mathrm{d}\Omega} = \frac{\mathrm{d}^2 p_\mathrm{i}}{\mathrm{d}E\,\mathrm{d}\Omega}\sum_{n=1}^{N-1}\binom{N}{n}\binom{N-n}{1} p_\mathrm{i}^{n-1} p_\mathrm{c} p_\mathrm{e}^{N-(n+1)}. \tag{A.4}$$

After simple algebra we get the final result for TI

$$\frac{\mathrm{d}^2\mathcal{P}_{c^1}}{\mathrm{d}E\,\mathrm{d}\Omega} = \frac{\mathrm{d}^2 p_\mathrm{i}}{\mathrm{d}E\,\mathrm{d}\Omega}\frac{1}{p_\mathrm{i}} N p_\mathrm{c}\left[(p_\mathrm{i}+p_\mathrm{e})^{N-1} - p_\mathrm{e}^{N-1}\right]. \tag{A.5}$$

If $p_\mathrm{i} \ll p_\mathrm{e}$, equations (A.3) and (A.5) lead to the following more transparent expressions

$$\text{ECC}: \frac{\mathrm{d}^2\mathcal{P}_{c^0}}{\mathrm{d}E\,\mathrm{d}\Omega} = N\frac{\mathrm{d}^2 p_\mathrm{i}}{\mathrm{d}E\,\mathrm{d}\Omega}(1-p_\mathrm{c})^{N-1} \tag{A.6a}$$

$$\text{TI}: \quad \frac{\mathrm{d}^2\mathcal{P}_{c^1}}{\mathrm{d}E\,\mathrm{d}\Omega} = N(N-1)\frac{\mathrm{d}^2 p_\mathrm{i}}{\mathrm{d}E\,\mathrm{d}\Omega} p_\mathrm{c}(1-p_\mathrm{c})^{N-2}. \tag{A.6b}$$

For a He target, equations (A.3) and (A.5) reduce to

$$\text{ECC}: \frac{\mathrm{d}^2\mathcal{P}_{c^0}}{\mathrm{d}E\,\mathrm{d}\Omega} = \frac{\mathrm{d}^2 p_\mathrm{i}}{\mathrm{d}E\,\mathrm{d}\Omega}(p_\mathrm{i}+2p_\mathrm{e}) \tag{A.7a}$$

$$\text{TI}: \quad \frac{\mathrm{d}^2\mathcal{P}_{c^1}}{\mathrm{d}E\,\mathrm{d}\Omega} = 2\frac{\mathrm{d}^2 p_\mathrm{i}}{\mathrm{d}E\,\mathrm{d}\Omega} p_\mathrm{c}. \tag{A.7b}$$

Integrating the above expressions over E and Ω, we obtain the following total electron emission probabilities

$$\mathcal{P}_{c^0} = 2p_i p_e + p_i^2 = P_{si} + P_{di} \tag{A.8a}$$

$$\mathcal{P}_{c^1} = 2p_i p_c = P_{ci}. \tag{A.8b}$$

Here we have used the notations P_{si}, P_{di} and P_{ci} for the integrated probabilities of the single, double and transfer ionization of He, respectively. These results are in accordance with those derived by Reinhold and Falcón (1986).

DDCSs for ECC and TI are obtained integrating equations (A.3) and (A.5) over the impact parameter

$$\frac{d^2\sigma_{c^{0,1}}}{dE\, d\Omega} = 2\pi \int_0^\infty b \frac{d^2\mathcal{P}_{c^{0,1}}(b)}{dE\, d\Omega}\, db. \tag{A.9}$$

References

Abrines R and Percival I C 1966 *Proc. Phys. Soc.* **88** 861

Barrachina R O 1997 *Nucl. Instrum. Methods* B **124** 198

Báder A, Sarkadi L, Víkor L, Kuzel M, Závodszky P A, Jalowy T, Groeneveld K O, Macri P A and Barrachina R O 1997 *Phys. Rev.* A **55** R14

Cocke C L 1993 *Review of Fundamental Processes and Applications of Atoms and Ions* ed C D Lin (Singapore: World Scientific) p 111

Crooks G B and Rudd M E 1970 *Phys. Rev. Lett.* **25** 1599

Crothers S F and McCann J F 1983 *J. Phys. B: At. Mol. Phys.* **16** 3229

Fainstein P D, Gulyás L and Salin A 1996 *J. Phys. B: At. Mol. Opt. Phys.* **29** 1225

Fainstein P D, Ponce V H and Rivarola R D 1991 *J. Phys. B: At. Mol. Opt. Phys.* **24** 3091

Fiol J, Rodríguez V D and Barrachina R O 2001 *J. Phys. B: At. Mol. Opt. Phys.* **34** 933

Garibotti C R and Miraglia J E 1980 *Phys. Rev.* A **21** 572

Garvey R H, Jackman C H and Green A E S 1975 *Phys. Rev.* A **12** 1144

Green A E S, Sellin D L and Zachor A S 1969 *Phys. Rev.* **184** 1

Jagutzki O, Koch R, Skutlartz A, Kelbch C and Schmidt-Böcking H 1991 *J. Phys. B: At. Mol. Opt. Phys.* **24** 993

Kövér Á, Sarkadi L, Pálinkás J, Berényi D, Szabó Gy, Vajnai T, Heil O, Groeneveld K O, Gibbons J and Sellin I A 1989 *J. Phys. B: At. Mol. Opt. Phys.* **22** 1595

Landau L D and Lifshitz E M 1975 *Quantum Mechanics* (Oxford: Pergamon)

Macri P A and Barrachina R O 1998 *J. Phys. B: At. Mol. Opt. Phys.* **31** 1303

Mergel V, Dörner R, Khayyat Kh, Achler M, Weber T, Jagutzki O, Lüdde H J, Cocke C L and Schmidt-Böcking H 2001 *Phys. Rev. Lett.* **86** 2257

Olson R E and Salop A 1976 *Phys. Rev.* A **14** 579

——1977 *Phys. Rev.* A **16** 531

Pálinkás J, Schuch R, Cederquist H and Gustafsson O 1989 *Phys. Rev. Lett.* **63** 2464

Plano V L, Haar R R, Tanis J A, Pálinkás J, Sarkadi L, Závodszky P A, Berényi D, Khemliche H, Prior M H and Schneider D 1994 *Nucl. Instrum. Methods* B **86** 181

Reinhold C O and Falcón C A 1986 *Phys. Rev.* A **33** 3859

Rudd M E, Toburen L H and Stolterfoht N 1976 *At. Data Nucl. Data Tables* **18** 413

Sarkadi L, Brinkmann U, Báder A, Hippler R, Tőkési K and Gulyás L 1998 *Phys. Rev.* A **58** 296

Sarkadi L, Kuzel M, Víkor L, Závodszky P A, Maier R, Berényi D and Groeneveld K O 1997 *Nucl. Instrum. Methods* B **124** 335

Sarkadi L, Pálinkás J, Kövér Á, Berényi D and Vajnai T 1989 *Phys. Rev. Lett.* **62** 527

Sarkadi L, Tőkési K and Barrachina R O 2000 *J. Phys. B: At. Mol. Opt. Phys.* **33** 847

Skutlartz A, Hagmann S and Schmidt-Böcking H 1988 *J. Phys. B: At. Mol. Opt. Phys.* **21** 3609

Tanis J A, Schneider D, Chantrenne S, Prior M H, Herrmann R, Hutton R and Schiwietz G 1990 *Phys. Rev.* A **42** 5776

Thomas L H 1927 *Proc. R. Soc.* **114** 561

Tőkési K and Mukoyama T 1994 *Bull. Inst. Chem. Res. Kyoto Univ.* **72** 62

Tőkési K, Sarkadi L and Mukoyama T 1997 *J. Phys. B: At. Mol. Opt. Phys.* **30** L123

Víkor L, Sarkadi L, Tanis J A, Báder A, Závodszky P A, Kuzel M, Groeneveld K O and Berényi D 1997 *Nucl. Instrum. Methods* B **124** 342

Víkor L, Sarkadi L, Tőkési K, Varga D, Penent F and Pálinkás J 1996 *Nucl. Instrum. Methods* B **114** 164

Víkor L, Závodszky P A, Sarkadi L, Tanis J A, Kuzel M, Báder A, Pálinkás J, Kamber E Y, Berényi D and Groeneveld K O 1995 *J. Phys. B: At. Mol. Opt. Phys.* **28** 3915

Závodszky P A, Kamber E Y, Woitke O, Tanis J A, Sarkadi L, Víkor L, Pálinkás J, Berényi D, Kuzel M and McDonald J 1995 *Proc. 19th Int. Conf. on the Physics of Electronic and Atomic Collisions (Whistler, Canada)* Abstracts of Contributed Papers 311

Závodszky P A, Sarkadi L, Tanis J A, Berényi D, Pálinkás J, Plano V L, Gulyás L, Takács E and Tóth L 1993 *Nucl. Instrum. Methods* B **79** 67

Zhu M, Haar R, Ferguson S M, Plano V L, Woitke O, Tanis J A, Sarkadi L, Pálinkás J, Závodszky P A and Berényi D 1995 *Nucl. Instrum. Methods* B **98** 351